

Experimental Communication

Cite

Karavyraki M, Gnaiger E, Porter RK (2022) Bioenergetics in human tongue pre-cancerous dysplastic oral keratinocytes and squamous cancer cells. *Bioenerg Commun* 2022.11.
<https://doi.org/10.26124/bec:2022-0011>

Author contributions

EG and RP conceived and planned the experiments. RKP supervised the project. MK performed the experiments. All authors discussed the results and contributed to the final manuscript.

Conflicts of interest

EG is founder and CEO of Oroboros Instruments

Received 2022-08-05

Reviewed 2022-09-05

Revised 2022-10-06

Accepted 2022-10-07

Published 2022-11-11

Open peer review

Christos Chinopoulos (editor)
 Jean Pierre Mazat (reviewer)
 Tuuli Kaambre (reviewer)

Keywords

oral squamous cancer cells;
 mitochondria;
 interleukin 6;
 dysplastic oral keratinocytes;
 oxygen consumption



Bioenergetics in human tongue pre-cancerous dysplastic oral keratinocytes and squamous cancer cells

Marilena Karavyraki ¹,  Erich Gnaiger ²,
 Richard K Porter ^{1*}

¹ School of Biochemistry, Trinity Biomedical Science Institute (TBSI), Trinity College Dublin, Ireland

² Oroboros Instruments, Innsbruck, Austria

* Corresponding author: rkporter@tcd.ie

Summary

In an endeavor to understand the metabolic phenotype behind oral squamous cell carcinomas, we characterized the bioenergetic profile of a human tongue derived cancer cell line (SCC-4 cells) and compared this profile to a pre-cancerous dysplastic oral keratinocyte (DOK) cell line also derived from human tongue. The human SCC-4 cancer cells had greater mitochondrial abundance but lower mitochondrial oxygen consumption rates than DOK cells. The lower oxygen consumption rate in SCC-4 cells can be partially explained by lower NADH-related enzymatic activity and lower mitochondrial complex 1 activity when compared to pre-cancerous DOK cells. In addition, SCC-4 cells have greater extracellular acidification rate (an index of glycolytic flux) when compared to DOK cells. In addition, treatment with recombinant human IL-6 (rhIL-6), known to drive *anoikis* resistance in SCC-4 cells but not DOK cells, impairs oxygen consumption in SCC-4 but not DOK cells, without affecting mitochondrial abundance. We conclude that SCC-4 cells have a less oxidative phenotype compared to DOK cells and that IL-6 attenuates mitochondrial function in SCC-4 cells while increasing glycolytic flux.

1. Introduction

Oral squamous cell carcinoma (OSCC) is the sixth most common cancer worldwide (Blatt et al 2017). The majority of oral cancer cases appear on the ventral-lateral edge of the tongue (40 %), floor of the mouth (30 %) and lower lip (Yellowitz et al 2000; Bagan et al 2010) and most commonly metastasizes to lymph nodes (Okura et al 2009). Surgical removal of the tumor, combined with radiation and chemotherapy, are the usual treatment regimens against OSCC, but they are only moderately successful (Moore et al 2000; Dong et al 2015). Thus, there is justification in seeking novel therapeutic targets for the treatment of oral cancer. *In vitro* models used to investigate OSCC include culturing squamous cell carcinoma-4 (SCC-4) cells, which were originally established from the tongue of a 55-year-old male (Rheinwald, Beckett, 1981). In regard to oral cancer, IL-6 production has been correlated with poor prognosis in oral carcinomas (Jinno et al 2015). In relation to SCC-4 cells in particular, it been demonstrated that SCC-4 cells have membrane bound IL-6 receptor (IL-6R/gp180) and that IL-6 drives *anoikis* resistance in these cells in an autocrine fashion and on addition of rhIL-6 (Karavyraki, Porter, 2022). Other studies have also demonstrated that IL-6 enhances migration of SCC-4 cells (Chuang et al 2014), proliferation (Chen et al 2012) and mediates osteoclastogenesis in SCC-4 cells (Tang et al 2008). In an endeavor, to understand the metabolic phenotype behind metastasis from oral squamous cell carcinomas, we characterized the bioenergetic profile of a human tongue derived cancer cell line (SCC-4 cells) (Rheinwald, Beckett, 1981) and compared this profile to a pre-cancerous dysplastic oral keratinocyte (DOK) cell line also derived from human tongue. We expected to see a less oxidative metabolic profile in the SCC-4 cancer cells, compared to the dysplastic cells (DOK) as would be predicted by the Warburg effect (Warburg 1956). In addition, we anticipated seeing a further decrease in SCC-4 cancer cell oxidative metabolism again commensurate with IL-6 driving a pro-cancer phenotype (Tang et al 2008; Chuang et al 2014; Karavyraki, Porter 2022).

2. Methods

2.1. DOK and SCC-4 cell lines

Dysplastic oral keratinocyte (DOK) cells were originally isolated from a piece of dorsal tongue of a 57-year-old male. DOK cells [cat# ECACC 94122104] are characterized as Caucasian derived epithelial adherent tongue dysplastic cells. Squamous cell carcinoma (SCC-4) cells were originally established from the tongue of a 55-year-old male [SCC-4 cat# ECACC 89062002]. Mycoplasma-free cells were grown in cell culture flasks in Dulbecco's Modified Eagle's Medium GlutaMAX cell culture medium (Gibco) with glucose (4.5 g/L) supplemented with 5 µg/mL hydrocortisone, 20 % (v/v) Fetal Bovine Serum (FBS) and penicillin-streptomycin (50 U/mL and 50 µg/mL; Gibco). Cells were grown at 37 °C in a humidified environment containing 95 % O₂ and 5 % CO₂. DOK and SCC-4 cells were passaged at least twice weekly depending on their levels of confluency (75-80 %) and were purchased from the European Centre of Authenticated Cell Culture. In terms of validity of comparability, all cells used in this study originated from the human buccal cavity and represent primary (PGK), pre-cancerous (DOK) and cancerous (SCC-4) cells, with the latter two being from the same tissue (tongue).

2.2. Oxygen consumption and extracellular acidification (Seahorse XF Analyzer)

The Seahorse XF Analyzer (Agilent, Santa Clara, US) provides multi-well plate analysis of two processes in real time, namely oxygen consumption rate OCR as an

indicator of cell respiration and extracellular acidification rate largely dependent on glycolytic processes (Gu et al 2020). Cellular oxygen consumption causes changes in the concentration of dissolved dioxygen O₂ in 'transient microchambers' as determined by solid-state fluorescent probes. Additions are injected pneumatically, limited to four sequential injections per well. The medium used for Seahorse experiments was XF Assay Medium supplemented with the desired concentration of glucose.

2.3. High-resolution respirometry (Oroboros Oxygraph-2k)

High-resolution respirometry by Oroboros Oxygraph-2k (O2k) *Coupling Control Protocol* (CCP) induces different coupling control states at constant substrate supply (Gnaiger 2020). The medium used in experiments was MiR05-kit (0.5 mM EGTA, 3 mM MgCl₂·6H₂O, 60 mM lactobionic acid, 20 mM taurine, 10 mM KH₂PO₄, 20 mM HEPES, 110 mM D-Sucrose, and 0.1 % (w/v) fatty-acid free BSA, pH 7.1), which does not contain energy substrates.

2.4. Biolog™ MitoPlate S-1 microplate analysis

Biolog™ MitoPlate S-1 microplates were used to screen various mitochondrial substrates that result in electron transport system activity. Substrates, coated on the bottom of the MitoPlate S-1, were dissolved using 30 µL per well of the assay mix, which is comprised of 2x Biolog MAS media, 6x Redox Dye MC, 24x saponin and sterile H₂O. Microplates were incubated in a sealed plastic bag for 1 hour prior to cell seeding at 37 °C to prevent evaporation of the medium and safeguard against atmospheric CO₂ of the incubator. Upon incubation, cells were trypsinized, centrifuged at 300 *g* for 5 minutes and seeded at a final cell concentration of 10⁶ x/mL in 30 µL of 1x Biolog MAS (30 000 cells per well). The plate was loaded in the OmniLog™ set at 37 °C to record Redox Dye decrease over time.

2.5. Citrate synthase activity

Citrate synthase enzyme activity was measured spectrophotometrically by a colorimetric coupled reaction, originally described by Srere (1969). The citrate synthase activity is determined by monitoring the rate of production of thionitrobenzoic acid (TNB) at a wavelength of 412 nm. Cells were subjected to three freeze thaw cycles in liquid nitrogen immediately prior to being assayed. Cell lysates were incubated at 30° C in a 1ml cuvette with Tris Buffer (0.2 M, pH 8.1), and the following reaction components were added in the corresponding concentrations; 5,5'- dithiobis- (2-nitrobenzoic acid) (DTNB) (0.1 mM), acetyl coenzyme A (0.3 mM) and Triton X (0.1 %). Freshly prepared oxaloacetate (0.5 mM) was added to initiate the reaction and an increase in the absorbance was monitored for 3 minutes. *Note:* our laboratory has previously demonstrated that citrate synthase activity gives an equivalent index of mitochondrial abundance when compared to immunoblotting for the mitochondrial outer membrane protein VDAC and the mitochondrial inner membrane protein cytochrome oxidase subunit 4 (Geoghegan et al 2017a).

2.6. NADH ubiquinone oxidoreductase (Complex I) activity

The activity of NADH-ubiquinone oxidoreductase (Complex I) was determined by monitoring the oxidation of NADH at 340 nm (Spinazzi et al 2012). Cell lysates were incubated at 30 °C in a 1 ml cuvette with potassium phosphate buffer (25 mM, pH 7.5), fatty acid free bovine serum albumin (BSA) (3 mg·mL⁻¹), KCN (0.3 mM) and NADH (0.1

mM). A blank rate was measured for 2 minutes before ubiquinone₁ (60 μM) was added to the cuvette to start the reaction and a decrease in absorbance was monitored for 3 minutes. Afterwards, rotenone (10 μM) was added to measure the rotenone-resistant activity and the rate was monitored for another 2 minutes. The specific Complex I activity is calculated as the rotenone-sensitive activity determined by subtracting the rotenone-resistant activity (with rotenone) from the total activity (without rotenone).

2.7. Protein determination using the bicinchoninic acid (BCA) assay

Quantification of protein concentrations in cell lysates was carried out using the Bicinchoninic Acid (BCA) assay as described by Smith et al (1985).

2.8. Statistical analysis

Statistical analyses were performed using the computer based mathematical package Graph Pad Prism 8.0 software. All results were expressed as mean \pm standard error of the mean for N number of independent experimental replicas [mean \pm SEM(N)] performed with at least three technical repeats ($n \geq 3$) For comparisons of two groups data were analyzed using a two-tailed unpaired student's *t*-test, while for comparisons of more than two groups, data were analyzed using one-way or two-way ANOVA followed by Tukey's or Sidak's or Bonferroni's multiple comparison tests were performed. Absolute *p*-values are given.

3. Results

3.1. Cellular metabolic/bioenergetic function in dysplastic oral keratinocytes (DOK) and immortal squamous cell carcinoma 4 (SCC-4) in suspension (Seahorse Flux Analyzer)

Significantly different total ROUTINE respiration rates R'_{tot} were measured for DOK and SCC-4 cells at 112 ± 3 (6) and 87 ± 6 (6) $\text{amol O}_2 \cdot \text{s}^{-1} \cdot \text{x}^{-1}$, respectively, where x is a single cell. Rotenone and antimycin A (1 μM and 3 μM final concentration, respectively) were used to determine the oxygen consumption not due to mitochondrial electron transfer (residual oxygen consumption R_{ox}) which was 18.3 ± 1.8 (6) and 21.1 ± 4.8 (6) $\text{amol O}_2 \cdot \text{s}^{-1} \cdot \text{x}^{-1}$, for DOK and SCC-4, respectively. ROUTINE respiration R was determined by subtracting R_{ox} from R'_{tot} and was significantly different at 93.5 ± 3.1 (6) and 65.6 ± 4.9 (6) $\text{amol O}_2 \cdot \text{s}^{-1} \cdot \text{x}^{-1}$ for DOK and SCC-4 cells, respectively (Figure 1A).

As demonstrated in Figure 1 A, DOK cells demonstrated significantly greater mitochondrial oxygen consumption OCR when compared to SCC-4 cells. In our endeavor to explain this differential oxygen consumption rate, we looked for differences in mitochondrial abundance. Cell lysates were used for citrate synthase activity measurements and activity was expressed per unit protein concentration. Interestingly and surprisingly, there was significantly higher mitochondrial abundance, as determined by citrate synthase activity, in SCC-4 cells when compared to DOK cells: 36.2 ± 1.7 (12) versus 15.2 ± 1.9 (9) $\text{nmol} \cdot \text{min}^{-1} \cdot \text{mg}^{-1}$ protein [mean \pm SEM (N)], respectively (Figure 1B).

The extracellular acidification rates (ECAR) under ROUTINE conditions, for DOK and SCC-4 cells were 11 ± 1 (6) and 25 ± 1 (6) $\text{mpH} \cdot \text{s}^{-1} \cdot \text{x}^{-1}$, respectively (Figure 1C). The extracellular acidification rate, an indirect indicator of glycolytic flux, was significantly higher in SCC-4 cells compared to DOK cells.

The ratio of extracellular acidification rate to mitochondrial oxygen consumption rates (ECAR/*R*) was calculated by dividing the ECAR to *R* and highlights the fact that SCC-4 cells [0.35 ± 0.02 (6)] are significantly more glycolytic than DOK cells [0.12 ± 0.01 (6), mean \pm SEM (*N*)] (Figure 1D).

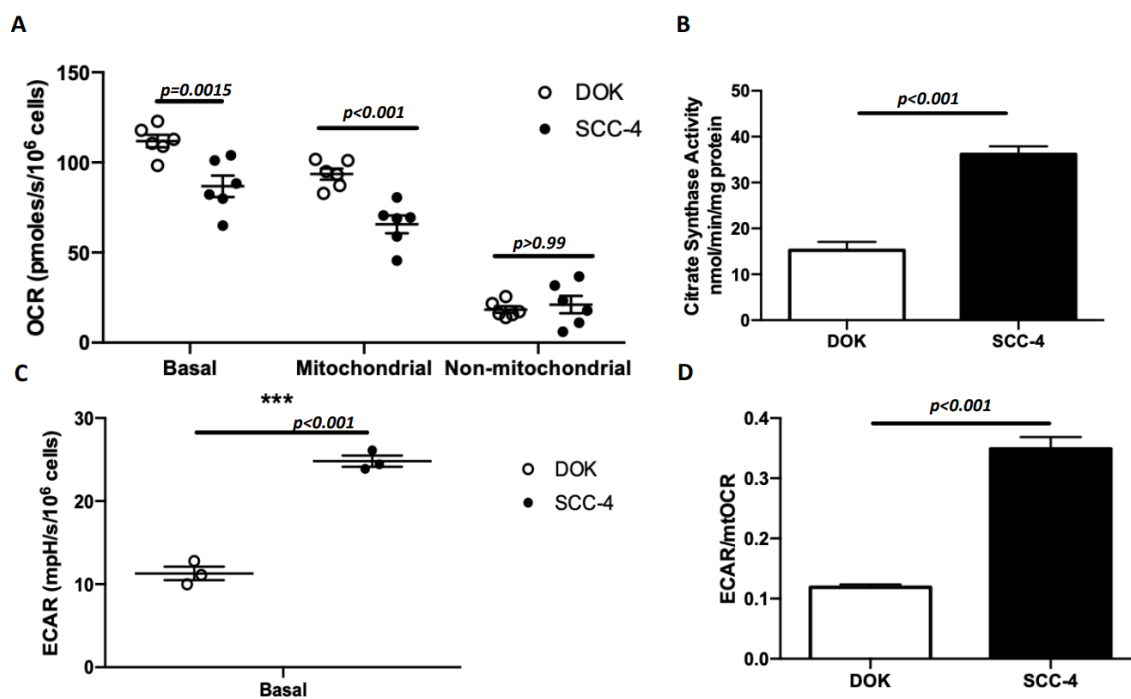


Figure 1. Cellular bioenergetics in dysplastic oral keratinocytes (DOK) and squamous cell cancer cells (SCC-4 cells) in the Seahorse Flux Analyzer.

(A) Cellular, mitochondrial and residual oxygen consumption rates, (B) citrate synthase activity, (C) extracellular acidification rate, (D) ECAR/*R* ratio, in DOK and SCC-4 cells. Values are expressed as mean \pm SEM (*N*).

3.2. Electron transfer systems in dysplastic oral keratinocytes (DOK) and immortal squamous cell carcinoma 4 (SCC-4) in suspension (Oroboros O2k)

The metabolic/bioenergetic function in dysplastic oral keratinocytes (DOK) cells and immortal squamous cell carcinoma 4 (SCC-4) cells, were compared using the Oroboros High-Resolution Respirometer O2k (Figure 2). This work used the 'Coupling Control Protocol' as suggested by the manufacturer, Oroboros Instruments. The results were as follows: After the pyruvate addition, respiration slightly increased in both cell lines but remained statistically insignificant from each other. In the absence of oligomycin, but after the uncoupler (CCCP) titration, respiration levels in SCC-4 cells were significantly lower when compared to DOK cells, revealing that the electron transport system (ETS) capacity in DOK cells is higher than that of SCC-4. In the presence of oligomycin which inhibits ATP synthesis, respiration in both DOK and SCC-4 cells was decreased, as expected. Figure 2A gives an example of the raw data output profile of the extended 'Coupling Control Protocol' used to compare the oxygen flow between the DOK and SCC-4 cell lines. The collated data for 6 amount of these experiments is given in Figure 2B. The data clearly demonstrate that oxygen consumption in the presence of pyruvate [68.4 ± 5.3 (6) $\text{amol O}_2 \cdot \text{s}^{-1} \cdot \text{x}^{-1}$], glucose [169.5 ± 15 (6) $\text{amol O}_2 \cdot \text{s}^{-1} \cdot \text{x}^{-1}$] and malate [180.2

± 13.2 (6) $\text{amol O}_2 \cdot \text{s}^{-1} \cdot \text{x}^{-1}$] is significantly greater in intact DOK cells when compared to intact SCC-4 cells [54.2 ± 5 , 102.1 ± 9 , 104.2 ± 7.4 (7) $\text{amol O}_2 \cdot \text{s}^{-1} \cdot \text{x}^{-1}$, respectively]. However, after cell permeabilization with digitonin, no significant differential rates were observed in the presence of succinate [DOK: 80.7 ± 16.1 (6) $\text{amol O}_2 \cdot \text{s}^{-1} \cdot \text{x}^{-1}$, SCC-4: 84.1 ± 5.6 (7) $\text{amol O}_2 \cdot \text{s}^{-1} \cdot \text{x}^{-1}$].

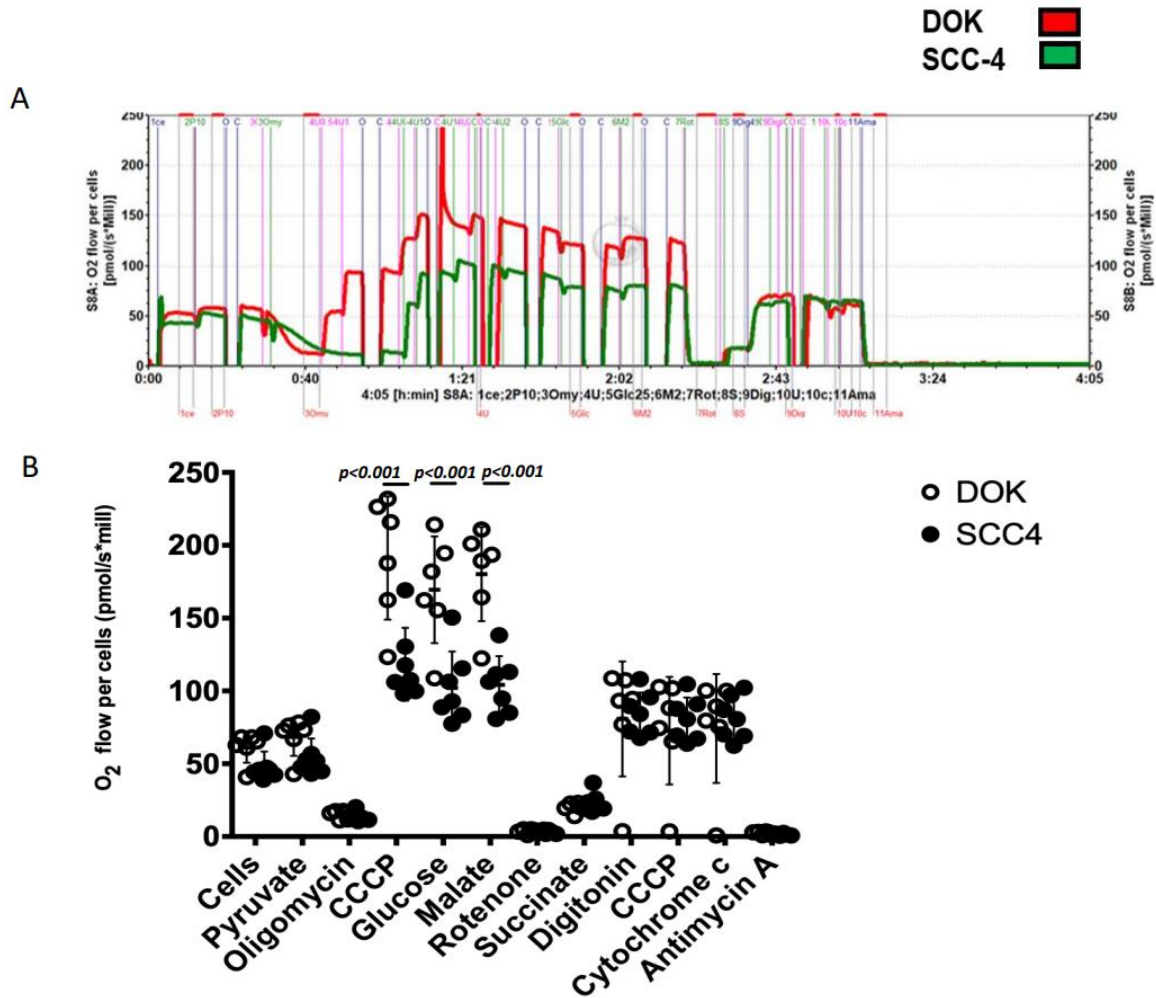


Figure 2. O2k analysis of DOK (red) vs SCC-4 (green) using the coupling control protocol. (A) Representative experiment from the Oxygraph O2k demonstrating the oxygen flow in (red) DOK and (green) SCC-4 cells using the “coupling control protocol”. **(B)** Collated data demonstrates that oxygen consumption in the presence of pyruvate, glucose and malate is significantly greater in intact DOK cells compared to intact SCC-4 cells. Results were plotted using Graphpad prism 8 and represent six and seven experiments performed in triplicate [mean \pm SEM (*n*)], *p*-values where shown indicate significance as measured by a two-way ANOVA with a Bonferroni multiple comparison post *hoc* test. Key: 1ce, cells-no substrate; 2P10, 10 mM pyruvate; 3U, 2.5 μM CCCP; 4Glc, 25 mM glucose; 5M, 2 mM malate; 6Rot, 5 μM rotenone; 7S, 10 mM succinate; 8Dig, 0.0041 $\mu\text{M} \times 2$ digitonin; 9U, 0.5 μM CCCP; 9c, 10 μM cytochrome *c*; 10Ama, 2.5 μM antimycin A.

3.3. Enzymatic metabolic/bioenergetic function in dysplastic oral keratinocytes (DOK) and immortal squamous cell carcinoma 4 (SCC-4) (Biolog™ Mitoplate and NADH dehydrogenase assays)

The mitochondrial metabolic phenotype of DOK and SCC-4 cells was investigated further using the phenotypic Mitoplate S-1 assay, to determine whether there were any differences in their mitochondrial enzyme activity (Figure 3A). DOK and SCC-4 were permeabilized with saponin so the substrates in the plate were immediately available to be metabolized. The key observation was that DOK cells appeared to have greater Krebs cycle enzyme activity compared to SCC-4 cells, as indicated by significantly greater metabolism of α -keto-glutaric acid ($p=0.015$), succinic acid ($p=0.018$) and L-malic acid ($p=0.016$), whereas SCC4 cells have greater glutamate and glutamine catabolism ($p=0.016$). Furthermore, there was a 2-fold ($p<0.01$) greater activity of mitochondrial NADH dehydrogenase (Complex I) associated with DOK cells compared to SCC4 cells (Figure 3B).

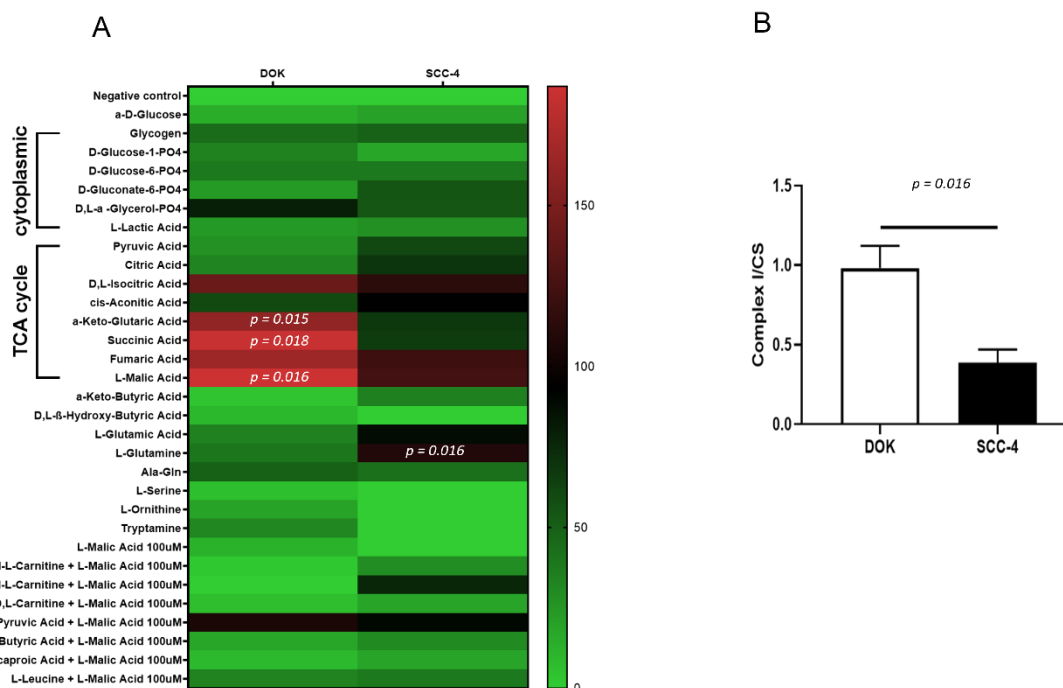


Figure 3. Mitochondrial substrate metabolism using the Biolog Mitoplate S-1 assay and the NADH dehydrogenase activity assay in DOK and SCC-4 cells. (A) Suspensions of DOK and SCC-4 cells were inoculated into the Mitoplate S-1 plates (Biolog, Hayward, CA) which contained 31 substrates. Negative controls had no substrate in the well. Wells containing α -D-glucose served as positive controls. Thresholds were set to disregard small and insignificant changes, and all wells that exceed this threshold are marked to denote differentially metabolized substrates for each cell line, which are described in the text. Heat map presents mitochondrial substrates utilization patterns of DOK and SCC-4 cells under non-starved conditions. Phenotypes that are lost are colored green and phenotypes that are gained are colored red; the exact relative values are given by a corresponding color as indicated on the color scales. Heat map shows collated data from 4 independent experiments. Statistical analysis was performed using the Holm-Sidak method. **(B)** NADH dehydrogenase activity was determined using the method of Spinazzi et al (2012). Statistical analysis was performed using ANOVA for 3 independent experiments performed in triplicate.

3.4. Effect of rhIL-6 on metabolic/bioenergetic function and respiratory profile of SCC-4 cells (Seahorse Flux Analyzer)

In light of the fact that SCC-4 cells express the IL-6/gp180-linked receptor, whereas DOK cells do not (Karavyraki, Porter, 2022), we set to determine whether added IL-6 affected bioenergetic function in these cells. Thus, recombinant human (rh) IL-6 (rhIL-6), was added to cells for a period of 24h (Figure 4), at a time and concentration known to be effective in promoting *anoikis* resistance in SCC-4 cells (Karavyraki, Porter, 2022). Figure 4A demonstrates that DOK cells were not significantly affected by addition of rhIL-6 [control value of 4 ± 0.2 (3) versus 3.7 ± 0.2 (3) pmol $O_2 \cdot s^{-1} \cdot mg^{-1}$ protein; mean \pm SEM (*N*)] for rhIL-6 treated cells. However, ROUTINE respiration was decreased significantly ($p \leq 0.001$) in SCC-4 cells following treatment with rhIL-6 from 3.6 ± 0.2 (3) to 1.6 ± 0 (3) pmol $O_2 \cdot s^{-1} \cdot mg^{-1}$ protein [mean \pm SEM (*N*)]. This decrease in oxygen consumption rate cannot be accounted for by any change in mitochondrial abundance as citrate synthase levels were equivalent in untreated SCC-4 cells and SCC-4 cells treated with rhIL-6 (Figure 4B). In a mirror image of what was observed for cellular oxygen consumption, extracellular acidification rates in SCC-4 cells were shown to significantly ($p \leq 0.001$) increase when rhIL-6 was added from 1.4 ± 0.01 (3) to 2.05 ± 0.01 (3) npH $\cdot s^{-1} \cdot mg^{-1}$ protein [mean \pm SEM (*N*)] (Figure 4C), whereas there was no significant effect of rhIL-6 treatment of DOK cells [1 ± 0.1 (3) npH $\cdot s^{-1} \cdot mg^{-1}$ protein for the control group versus 1.2 ± 0.1 (3) npH $\cdot s^{-1} \cdot mg^{-1}$ protein for the rhIL-6 treated DOK cells]. A secondary plot of the ECAR/R ratio for DOK and SCC-4 cells accentuates the significant effect of rhIL-6 on ECAR/R ratio for SCC-4 cells, with no significant effect of rhIL-6 on ECAR/R ratio in DOK cells (Figure 4D).

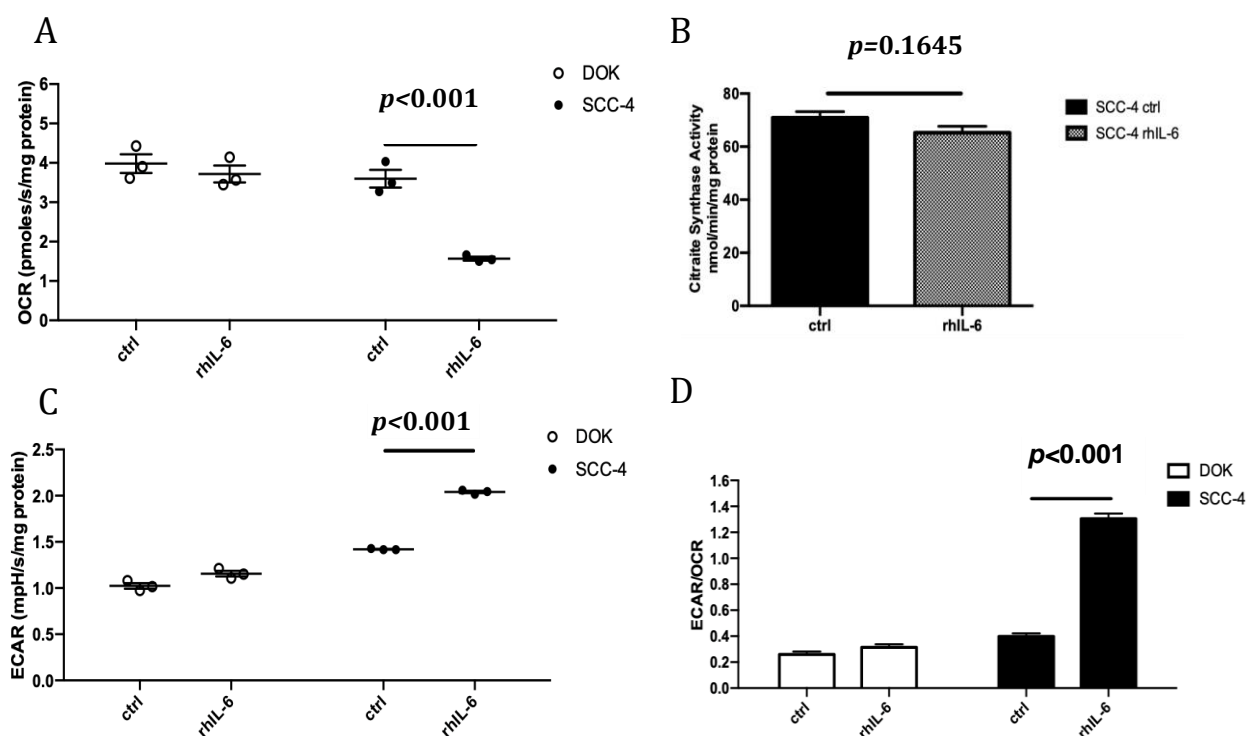


Figure 4. The effect of added rhIL-6 on oxygen consumption rate in DOK and SCC-4 cells. (A) Cellular OCR, **(B)** citrate synthase activity, an index of mitochondrial density, **(C)** cellular ECAR in DOK and SCC-4 cells treated with or without rhIL-6, **(D)** ECAR/R ratio for DOK and SCC-4 cells treated with or without rhIL-6.

3.5. Effect of rhIL-6 on metabolic/bioenergetic function and respiratory profile of SCC-4 cells in suspension (Oroboros O2k)

To explore the site of inhibition upon rhIL-6 treatment, we again employed the *Coupling Control Protocol* with the Oroboros O2k. SCC-4 cells were seeded, following treatment with 30 ng/mL rhIL-6 or left untreated (control) for 24 hours. The collated data for the experiments are given in Figure 5. The oxygen consumption in intact untreated SCC-4 cells was significantly ($p = 0.0022$) greater than in SCC-4 treated with rhIL-6, confirming the data in Figure 4. Following pyruvate addition, oxygen consumption rate was again significantly greater ($p = 0.0022$) in intact untreated SCC-4 cells compared to intact SCC-4 cells treated with rhIL-6. No significant differences in oxygen consumption rate were observed, between untreated and rhIL-6 treated SCC-4 cells, after subsequent addition of uncoupler CCCP, glucose, malate, rotenone, succinate, digitonin, more uncoupler or cytochrome *c*. Subsequent addition of antimycin A inhibited mitochondrial oxygen consumption as expected.

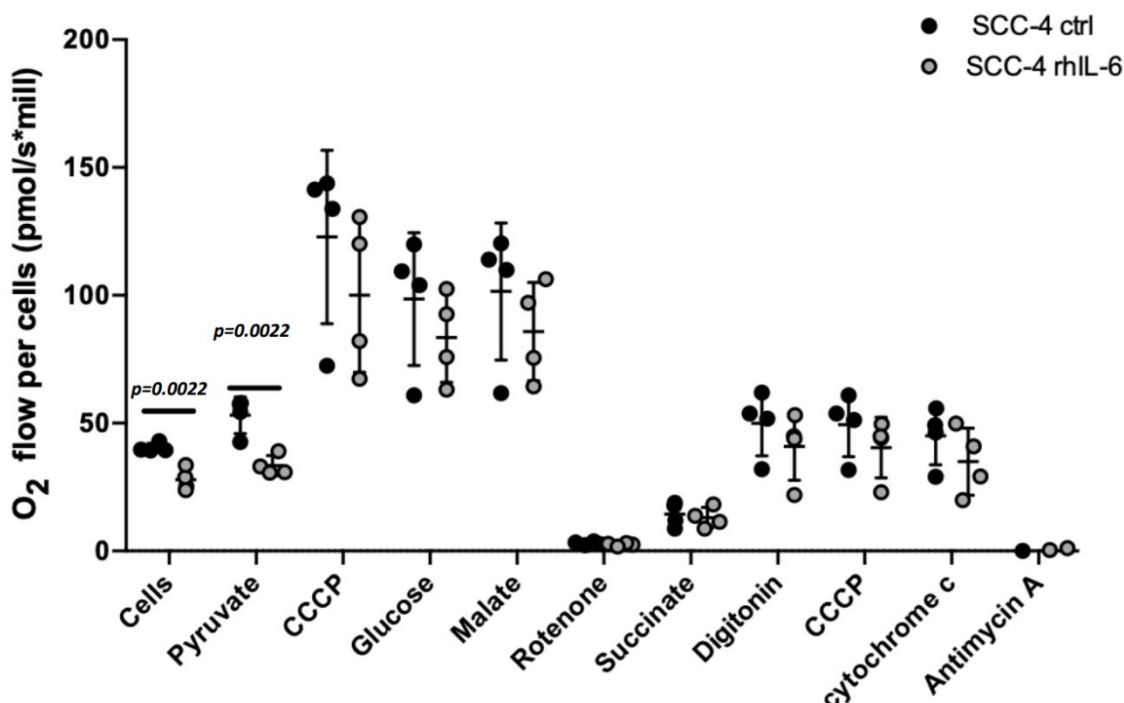


Figure 5. Collated data of oxygen flow in SCC-4 untreated and treated with rhIL-6 as a function of substrates (coupling control protocol). Intact SCC-4 cells treated with externally added 30 ng/mL rhIL-6 for 24 hours demonstrated significantly decreased oxygen consumption compared to non-treated controls, in the absence of substrate (1ce) and in the presence of 10 mM pyruvate (2P10). Oxygraph O2k experiments were performed using the coupling control protocol. Results were plotted using Graphpad prism. Results represent three experiments performed [mean ± SEM (3)]. Data were analyzed using two-way ANOVA with a Bonferroni multiple comparison post-test.

4. Discussion

The bioenergetic profiles of human tongue dysplastic oral keratinocytes (DOK) and squamous cell carcinoma (SCC-4) cells were investigated and compared. Based on Warburg's (1956) *ex vivo* observations, one might have expected to observe little or no oxidative metabolism and a higher relative glycolytic flux in cancerous SCC-4 cells

compared to pre-cancerous DOK cells. It was observed that both DOK and SCC-4 cells have significant mitochondrial oxygen consumption indicating that the mitochondria are active and performing oxidative phosphorylation. Indeed, the cellular and mitochondrial oxygen consumption rates of pre-cancerous DOK cells was ~1.4-fold those of cancerous SCC-4 cells. Thus, in the context of Warburg's observation, it is clear there is no absolute mitochondrial dysfunction in the cancerous SCC-4 but clearly there is a lower oxidative metabolism in SCC-4 cells compared to the pre-cancerous DOK cells.

In an attempt to explain the greater mitochondrial oxygen consumption in DOK cells compared to SCC-4 cells, we measured mitochondrial abundance, as indexed by citrate synthase activity. Surprisingly, it was observed that SCC-4 cells have significantly greater (~2.3-fold) mitochondrial abundance when compared to DOK cells. Thus, if one expressed cellular oxygen consumption per unit mass of mitochondria, there is a ~3-fold lower oxygen consumption rate in SCC-4 cells compared to DOK cells. Taking into account the mitochondrial oxygen consumption rate data alone or in combination with mitochondrial abundance, the data would suggest that there is either (a) some suppression or dysfunction of mitochondrial function in SCC-4 cells compared to DOK cells or (b) that substrate supply to mitochondria in SCC-4 cells is decreased compared to DOK cells.

It was also observed that there was greater (~ 2.3-fold) extracellular acidity (ECAR) in SCC-4 cells compared to DOK cells. ECAR is an index of glycolytic flux due to lactic acid production and release from cells resulting in acidification of the medium. This greater glycolytic flux in SCC-4 cells would be consistent with the aforementioned sub-optimal mitochondrial activity in those cells (compared to DOK cells) and again would be characteristic of cancer tissue (Warburg, 1957) and cancer cells (Sun et al 2019).

The authors could find no other published data reporting mitochondrial oxygen consumption rates for DOK cells, but for SCC-4 cells, the absolute oxygen consumption rate data and ECAR in this study compares well with published data (Duicu et al 2018; Guo et al 2020). Furthermore, the observation that there was significant mitochondrial oxygen consumption in SCC-4 cancer cells is not unusual in that many laboratories, including our own, has demonstrated significant oxidative phosphorylation occurring in various cancer cell lines such as non-small lung cancer cells, mesothelioma cells (Geoghegan et al 2017a), neuroblastoma cells (Geoghegan et al 2017b) and triple negative breast cancer cells (O'Neill et al 2019).

Endeavors to understand why mitochondria in SCC-4 cells were operating sub-optimally, compared to those in DOK cells, led to detailed bioenergetic analysis of cellular bioenergetic function using the coupled control protocol designed for the Oroboros Respirometer. It was observed that there was greater NADH-related substrate activity and mitochondrial Complex I activity in DOK cells compared to SCC-4 cells. This observation is again consistent with the aforementioned greater oxygen consumption rates observed in DOK cells compared to SCC-4 cells. Furthermore, the BiologTM Microarray data compliments that for the coupled control protocol from the Oroboros Respirometer in that DOK cells have greater NADH-related activity compared to SCC-4 cells. However, it should be pointed out there that is significant oxidative metabolism occurring in SCC4 cells with approximately two-thirds of ATP coming from oxidative phosphorylation, as estimated from OCR and ECAR fluxes.

Finally, in light of the fact that added rhIL-6 has been demonstrated to enhance *anoikis resistance* in SCC-4 cells (Karavyraki, Porter, 2022), it was a logical step to determine whether added rhIL-6 could affect bioenergetic function in these cells. It was

demonstrated that added rhIL-6 significantly decreased oxygen consumption rates by half and significantly increased extracellular acidification rates (~3-fold) in SCC-4 cells. This decrease in oxygen consumption on addition of rhIL-6 was not due to differences in mitochondrial abundance and persisted when pyruvate was added to cells without substrate, indicating that rhIL-6 affected (a) substrate supply to mitochondria or (b) attenuated mitochondrial function. It is interesting to note IL-6 has been demonstrated to decrease mitochondrial oxygen consumption in mouse myotubes (Abid et al 2020) but has no effect on mitochondrial consumption in rat hepatocytes (Berthiaume et al 2003). Overall, our prediction that there would be a less oxidative metabolic profile in the SCC-4 cancer cells, compared to the dysplastic cells (DOK), is evident. Furthermore, it appears that IL-6 is driving a less oxidative metabolic phenotype in these already cancerous SCC-4 cells, again as we would have predicted from our knowledge that IL-6 drives *anoikis* resistance (Karavyraki, Porter, 2022).

Abbreviations

CCCP	carbonyl cyanide m-chlorophenyl	IL-6	interleukin-6
DOK	dysplastic oral keratinocytes	OCR	oxygen consumption rate
ECAR	extracellular acidification rate	OSCC	oral squamous cell cancer
FBS	fetal bovine serum	SCC	squamous cancer cells

Acknowledgements

Marie Curie Grant TRACT 721906 H2020-MCSA-ITN 2016; COST Action CA15203 (2016-2021) MitoEAGLE.

References

- Abid H, Ryan ZC, Delmotte P, Sieck GC, Lanza IR (2020) Extramyocellular interleukin-6 influences skeletal muscle mitochondrial physiology through canonical JAK/STAT signaling pathways. <https://doi.org/10.1096/fj.202000965RR>
- Bagan J, Sarrion G, Jimenez Y (2010) Oral cancer: clinical features. <https://doi.org/10.1016/j.oraloncology.2010.03.009>
- Berthiaume F, MacDonald AD, Kang, YH, Yarmush, ML (2003) Control analysis of mitochondrial metabolism in intact hepatocytes: effect of interleukin-1 β and interleukin-6. [https://doi.org/10.1016/s1096-7176\(03\)00010-7](https://doi.org/10.1016/s1096-7176(03)00010-7)
- Blatt S, Krüger M, Ziebart T, Sagheb K, Schiegnitz E, Goetze E, Al-Nawas B, Pabst AM (2017) Biomarkers in diagnosis and therapy of oral squamous cell carcinoma: A review of the literature. <https://doi.org/10.1016/j.jcms.2017.01.033>
- Chen M-F, Wang W-H, Lin P-Y, Lee K-D, Chen W-C (2012) Significance of the TGF- β 1/IL-6 axis in oral cancer. <https://doi.org/10.1042/CS20110434>
- Chuang J-Y, Huang Y-L, Yen W-L, Chiang I-P, Tsai M-H, Tang C-H (2014) Syk/JNK/AP-1 Signaling pathway mediates interleukin-6-promoted cell migration in oral squamous cell carcinoma. <https://doi.org/10.3390/ijms15010545>
- Duicu OM, Pavel IZ, Borcan F, Muntean DM, Cheversean A, Bratu EA, Rusu LC, Karancsi OL (2018) Characterization of the eugenol effects on the bioenergetic profile of SCC-4 human squamous cell carcinoma cell line. <https://doi.org/10.37358/RC.18.9.6577>
- Jinno T, Kawano S, Maruse Y, Matsubara R, Goto Y, Sakamoto T, Hashiguchi Y, Kaneko N, Tanaka H, Kitamura R, Toyoshima T, Jinno A, Moriyama M, Oobu K, Kiyoshim T, Nakamura S (2015) Increased expression of interleukin-6 predicts poor response to chemoradiotherapy and unfavorable prognosis in oral squamous cell carcinoma. <https://doi.org/10.3892/or.2015.3838>

- Geoghegan F, Buckland RJ, Rogers ET, Khalifa K, O'Connor EB, Rooney MF, Behnam-Motlagh P, Nilsson TK, Grankvist K, Porter RK (2017a) Bioenergetics of acquired cisplatin resistant H1299 non-small cell lung cancer and P31 mesothelioma cells. <https://doi.org/10.18632/oncotarget.21885>
- Geoghegan F, Chadderton N, Jane Farrar G, Zisterer DM, Porter RK (2017b) Direct effects of phenformin on metabolism/bioenergetics and viability of SH-SY5Y neuroblastoma cells. <https://doi.org/10.3892/ol.2017.6929>
- Gnaiger E (2020) Mitochondrial pathways and respiratory control. An introduction to OXPHOS analysis. 5th ed. <https://doi.org/10.26124/bec:2020-0002>
- Gu X, Ma Y, Liu Y, Wan Q (2020) Measurement of mitochondrial respiration in adherent cell by Seahorse XF96 Cell Mito Stress Test. <https://doi.org/10.1016/j.xpro.2020.100245>
- Guo J, Su Y, Zhang M (2020) Circ_0000140 restrains the proliferation, metastasis and glycolysis metabolism of oral squamous cell through upregulating CDC73 via sponging miR-182-5p, <https://doi.org/10.1186/s12935-020-01501-7>
- Karavyraki M, Porter RK (2022) Evidence of a role for interleukin-6 in anoikis resistance in oral squamous cell carcinoma. <https://doi.org/10.1007/s12032-022-01664-5>
- Moore SR, Johnson NW, Pierce AM, Wilson DF (2000) The epidemiology of tongue cancer: A review of global incidence. <https://doi.org/10.1111/j.1601-0825.2000.tb00105.x>
- Okura M, Aikawa T, Sawai N, Lida S, Kogo M (2009) Decision analysis and treatment threshold in a management for the NO neck of the oral cavity carcinoma <https://doi.org/10.1016/j.oraloncology.2009.03.013>
- O'Neill S, Porter RK, McNamee N, Martinez VG, O'Driscoll L (2019) 2-Deoxy-D-Glucose inhibits aggressive triple-negative breast cancer cells by targeting glycolysis and the cancer stem cell phenotype. <https://doi.org/10.1038/s41598-019-39789-9>
- Rheinwald JG, Beckett MA (1981) Tumorigenic keratinocyte lines requiring anchorage and fibroblast support cultures from human squamous cell carcinomas. <https://pubmed.ncbi.nlm.nih.gov/7214336>
- Smith PK, Krohn RI, Hermanson GT, Mallia AK, Gartner FH, Provenzano MD, Fujimoto EK, Goeke NM, Olson BJ, Klenk DC (1985) Measurement of protein using bicinchoninic acid. [https://doi.org/10.1016/0003-2697\(85\)90442-7](https://doi.org/10.1016/0003-2697(85)90442-7)
- Spinazzi M, Casarin A, Pertegato V, Salviati L, Angelini C (2012) Assessment of mitochondrial respiratory chain enzymatic activities on tissues and cultured cells. <https://doi.org/10.1038/nprot.2012.058>
- Srere (1969) Citrate synthase: [EC 4.1.3.7. Citrate oxaloacetate-lyase (CoA-acetylating)]. [https://doi.org/10.1016/0076-6879\(69\)13005-0](https://doi.org/10.1016/0076-6879(69)13005-0)
- Sun H, Chen L, Cao S, Liang Y, Xu Y (2019) Warburg effects in cancer and normal proliferating cells: two tales of the same name. <https://doi.org/10.1016/j.gpb.2018.12.006>
- Tang C-H, Chuang J-Y, Fong Y-C, Maa M-C, Way T-D, Hung C-H (2008) Bone-derived SDF-1 stimulates IL-6 release via CXCR4, ERK and NF-kB pathways and promotes osteoclastogenesis in human oral cancer cells. <https://doi.org/10.1093/carcin/bgn045>
- Warburg O (1956) On the origin of cancer cells. <https://doi.org/10.1126/science.123.3191.309>
- Yellowitz JA, Horowitz AM, Drury TF, Goodman HS (2000) Survey of U.S. dentists' knowledge and opinions about oral pharyngeal cancer. <https://doi.org/10.14219/jada.archive.2000.0239>

Copyright © 2022 The authors. This Open Access peer-reviewed communication is distributed under the terms of the Creative Commons Attribution License, which permits unrestricted use, distribution, and reproduction in any medium, provided the original authors and source are credited. © remains with the authors, who have granted BEC an Open Access publication license in perpetuity.

